^{11}C-Acetate PET Imaging in Hepatocellular Carcinoma and Other Liver Masses

Chi-Lai Ho, MBBS[1,2]; Simon C.H. Yu, MBBS[3]; and David W.C. Yeung, MBBS[1,2]

[1]Department of Nuclear Medicine and PET, Hong Kong Sanatorium and Hospital, Hong Kong, China; [2]Department of Radiology, University of Hong Kong, Hong Kong, China; and [3]Department of Diagnostic Radiology and Organ Imaging, Prince of Wales Hospital, Hong Kong, China

It is well known that ^{18}F-FDG PET has a high average false-negative rate of 40%–50% in the detection of hepatocellular carcinoma (HCC). This is not an acceptable accuracy, particularly in countries where this tumor is prevalent. In this study, we evaluated prospectively the characteristics of ^{11}C-acetate and ^{18}F-FDG metabolism in HCC and other liver masses. **Methods:** Fifty-seven patients were recruited into this study, with masses consisting of 39 HCC; 3 cholangiocarcinomas; 10 hepatic metastases from lung, breast, colon, and carcinoid primary malignancies; and 5 benign pathologies, including focal nodular hyperplasia (FNH), adenoma, and hemangioma. All patients, except 2 with typical findings of hemangioma and 3 clinically obvious metastases, were confirmed histopathologically by liver biopsy or resection. All patients fasted for at least 6 h and blood glucose concentration was measured before they underwent dual PET radiopharmaceutical evaluation of the upper abdomen with ^{11}C-acetate and ^{18}F-FDG. **Results:** In the subgroup of HCC patients with the number of lesions $\leq$ 3 (32 patients; 55 lesions; mean size $\pm$ SD, 3.5 $\pm$ 1.9 cm), the sensitivity of detection by ^{11}C-acetate is 87.3% (^{11}C-acetate maximum SUV [SUV_{max}] = 7.32 $\pm$ 2.02, with a lesion-to-normal liver ratio of 1.96 $\pm$ 0.63), whereas the sensitivity of detection by ^{18}F-FDG is only 47.3%, and 34% lesions show uptake of both tracers. None of the lesions was negative for both tracers (100% sensitivity using both tracers). In some lesions and in the subgroup of HCC patients (n = 7) with multifocal or diffuse disease, dual-tracer uptake by different parts of the tumor is demonstrated. Histopathologic correlation suggests that the well-differentiated HCC tumors are detected by ^{11}C-acetate and the poorly differentiated types are detected by ^{18}F-FDG. All 16 non-HCC malignant (cholangiocarcinoma and metastatic) liver lesions do not show abnormal ^{11}C-acetate metabolism. Of the benign liver lesions, only FNH shows mildly increased ^{11}C-acetate activities (^{11}C-acetate SUV_{max} = 3.59, with a lesion-to-normal liver ratio of 1.25). **Conclusion:** ^{11}C-Acetate has a high sensitivity and specificity as a radiotracer complementary to ^{18}F-FDG in PET imaging of HCC and evaluation of other liver masses.

Key Words: ^{11}C-acetate; PET; hepatocellular carcinoma

J Nucl Med 2003; 44:213–221

Hepatocarcinoma (HCC) is 1 of the top 3 causes of cancer death in many Asian countries, including China, Taiwan, Singapore, and Japan. The disease is also believed to be showing an upward trend in America because of the increasing frequency of hepatitis C viral infection (*1*), and it is also a common cause of cancer death among Asian immigrants. The predisposing factors include hepatitis B antigen carrier status, chronic hepatitis C, cirrhosis, alcohol, and other hepatotoxins. Basic investigation includes a screening blood test for elevated α-fetoprotein concentration. The conventional method of detection for HCC is by structural imaging, most commonly and economically by sonography, followed by contrast CT and MRI (*2–4*). In the past decades, the use of PET, with ^{18}F-FDG as the functional probe, has been found to be successful in the evaluation of many forms of solid malignancies. However, it is well known that ^{18}F-FDG is far from being a universal tracer on the basis of the understanding that tumor kinetics may vary and increased glycolysis may not be the preferred kinetic pathway in some tumors. It is understood that HCC is one of the known tumors that may exhibit a net glycolysis similar to or even lower than that of normal liver parenchyma and therefore may escape detection (*5–13*). The average reported false-negative rate using ^{18}F-FDG PET in HCC approaches 40%–50% (*6,10,11,14*). In countries where this tumor is prevalent, this low sensitivity has been a major weakness of ^{18}F-FDG PET in the evaluation of liver masses. Several research studies in the recent years have demonstrated that ^{11}C-acetate may be a useful tracer for urologic tumors (*15,16*). Because there are no data in the literature regarding the use of this tracer in liver masses, this study was designed to evaluate prospectively the characteristics of ^{11}C-acetate metabolism in HCC and some selective liver pathology. Its potential use as a radiotracer complementary to ^{18}F-FDG in the detection of HCC was investigated.

MATERIALS AND METHODS

Patients

Fifty-seven patients (37 men, 20 women; age range, 27–88 y; mean age, 60 y) with liver masses were recruited into this study,

Received Mar. 6, 2002; revision accepted Jul. 9, 2002.

For correspondence or reprints contact: Chi-Lai Ho, MBBS, Department of Nuclear Medicine and PET, Hong Kong Sanatorium and Hospital, 2 Village Rd., Happy Valley, Hong Kong, China.

E-mail: garrettho@hksh.org.hk

with masses consisting of 39 HCC, 3 cholangiocarcinomas (primary adenocarcinoma), 2 metastases from lung, 3 metastases from colon, 2 metastases from breast, 3 metastatic carcinoid tumors, 2 focal nodular hyperplasia (FNH), 1 adenoma, and 2 hemangiomas. All patients, except 2 with typical findings of hemangioma and 3 clinically obvious metastases, were confirmed histopathologically by liver biopsy 1–3 wk before or after PET imaging or by operative tumor resection. All patients underwent PET imaging of the upper abdomen with ^{11}C-acetate and ^{18}F-FDG on the same day or within 7 d between the 2 scans. All patients fasted for at least 6 h and blood glucose concentration was measured before imaging. Forty patients were hepatitis B antigen positive.

^{11}C-Acetate Synthesis, Injection, and Imaging

^{11}C-Acetate was prepared by modifying the methodology and setup proposed by Norenberg et al. (*17*). A dose of 555 MBq (15 mCi) ^{11}C-acetate was administered intravenously, and regional imaging of the upper abdomen in 2 positions was performed at 10 min after injection using an ECAT EXACT 47 PET scanner (model 921; CTI/Siemens, Inc., Knoxville, TN). The axial field of view was 16.2 cm. Both transmission and emission scans were obtained with a total of 10-min acquisition time for each position. Attenuation correction was performed with the standardized ordered-subsets expectation maximization technique. Reconstructed transaxial spatial resolution was about 4.4 mm. These images were compared with the anatomic images (CT or MRI).

^{18}F-FDG Synthesis, Injection, and Imaging

^{18}F-FDG synthesis was based on the standard technique of Hamacher et al. (*18*) (CTI Corp. chemical synthesizer). A dose of 37–555 MBq (10–15 mCi) ^{18}F-FDG was injected intravenously. For those patients undergoing the same-day protocol, ^{18}F-FDG was injected at 10–15 min after ^{11}C-acetate imaging (40–45 min after initial ^{11}C-acetate injection). Regional imaging of the upper abdomen of the same patient began at 45–60 min after ^{18}F-FDG administration. This allowed a total of 85–105 min after the initial injection of ^{11}C-acetate—thus, >4–5 decay half-lives of ^{11}C (20 min). For the first few cases with positive ^{11}C-acetate uptake in the tumor lesions, imaging at 85–100 min before ^{18}F-FDG injection was performed to confirm little or no significant residual activities before this technique was adopted for all subsequent patients (the most intense pancreatic uptake of ^{11}C-acetate was not seen on all ^{18}F-FDG PET images). Instrumentation, imaging, reconstruction, and semiquantitative analysis were similar to the specifications as stated above.

Interpretation Criteria and Statistical Analysis

The hepatic masses were referred to the CT or MR images for lesion-to-lesion comparison. A lesion was regarded as positive for ^{18}F-FDG or ^{11}C-acetate on the basis of visual judgment of the degree of increased metabolism, supported by calculation of the standardized uptake value (SUV). A lesion was considered negative for the PET tracer (^{18}F-FDG or ^{11}C-acetate) when it was isointense with nontumor tissue by visual inspection, supported by a lesion-to-liver SUV ratio of <1.20. Both maximum and average values were calculated. The region of interest (ROI) was drawn automatically at 75% threshold of the maximum lesion count around the tumor. The same ROI was used to evaluate the SUV of nontumor liver tissue in the same patient. For those patients whose lesion was seen with only 1 type of PET tracer, the same ROI was applied at the same level on the transaxial images of the other PET tracer after direct visual alignment of both sets of images. For the subgroup of patients with multifocal or diffuse disease, the ROI was drawn either automatically or manually around the representative lesions or areas. In some of these patients with advanced or infiltrative disease, semiquantitative evaluation was not possible or was possible only in some lesions, and nontumor tissue could be defined only as liver tissue with no apparent tumor on CT or MRI and on PET imaging. The biopsy sites were identified if biopsies were performed before PET imaging. Statistical analysis with an unpaired Student *t* test was performed on (a) the ^{11}C-acetate–positive HCC lesions to check for any significant difference with the benign lesions, (b) the non-HCC malignant lesions with normal liver tissue, and (c) the average lesion-to-liver ratios among the HCC patients with ≤3 tumor lesions (group Ia, as defined below) according to cellular differentiation. Partial-volume effect correction was not performed because only 3 lesions in this study were between 1.7 and 2.0 cm in size.

RESULTS

These 57 patients were divided into 3 groups: Group I consisted of 39 patients with biopsy-confirmed HCC; group II consisted of 13 patients with non-HCC malignancies (3 cholangiocarcinomas, 10 secondary tumors in liver); group III consisted of 5 patients with benign liver lesions (hemangioma, adenoma, FNH). Group I patients were further subdivided into 2 groups: group Ia (n = 32), those patients who had ≤3 lesions and disease was confined within the hepatic parenchyma; and group Ib (n = 7), those patients with >3 lesions, including those with diffusely infiltrating or multifocal disease, vascular invasion, and extrahepatic metastasis.

In group Ia, there were 32 patients with a total of 55 hepatic lesions. Of these 55 HCC lesions, 29 were positive only for ^{11}C-acetate (Fig. 1A), 7 were positive only for ^{18}F-FDG (Fig. 1B), and 19 were positive for both (Fig. 1C). Lesion size ranged from 1.7 to 11.1 cm (mean size, 3.5 ± 1.9 cm). On the basis of this subgroup statistics, the sensitivity for detection of HCC by ^{11}C-acetate was 87.3% (lesions positive only for ^{11}C-acetate plus lesions positive for both ^{11}C-acetate and ^{18}F-FDG; n = 48). Whereas for ^{18}F-FDG, the sensitivity for detection of HCC was only 47.3% (lesions positive only for ^{18}F-FDG plus lesions positive for both; n = 26). Results are summarized in Table 1. About 34.5% (n = 19) of these HCC lesions showed increased metabolism of both radiotracers, and some lesions appeared to be complementary (different tracer uptake in different parts of the same tumor lesion, as shown in a patient in Fig. 2). The average ^{11}C-acetate maximum SUV [SUV_{max}] in group Ia HCC lesions was 7.32 ± 2.02 (mean ± SD; range, 4.11–13.28), with an average lesion-to-liver ratio of 1.96 ± 0.63 (SE = 0.11 at $t_{0.025}$).

The observation that these 2 tracers were complementary in some lesions was also demonstrated by the 7 patients in group Ib—that is, the patient subgroup with advanced, metastatic, or late-stage disease (Fig. 3). Six of these patients showed poorly differentiated or moderate-to-poorly differentiated pathology. Systematic quantitative evaluation of this group of patients was not possible because many

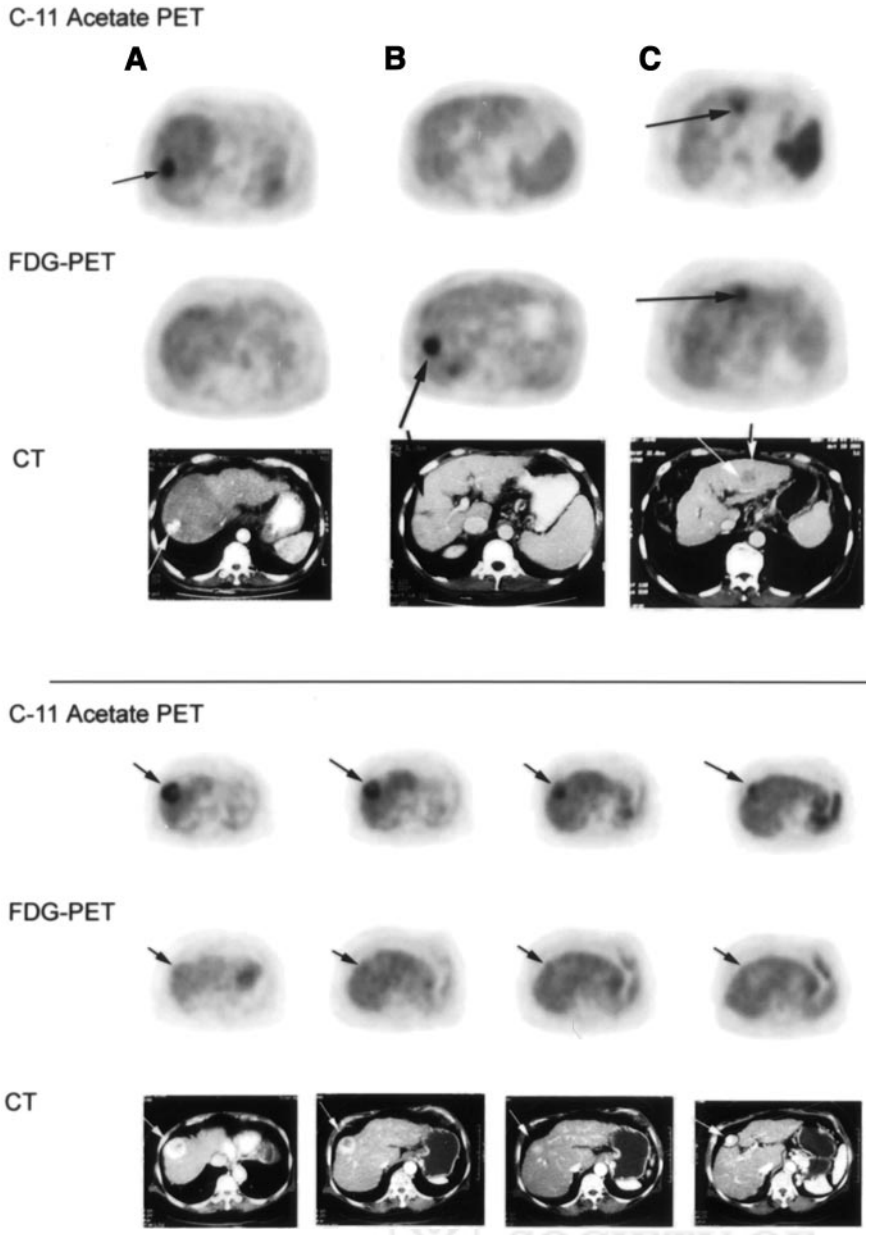

FIGURE 1. Transaxial sections of liver in 4 patients compare ^{11}C-acetate PET with ^{18}F-FDG PET and CT. (Top) Left patient (A) has well-differentiated HCC in right lobe that shows markedly increased ^{11}C-acetate metabolism but no ^{18}F-FDG accumulation. Middle patient (B) has poorly differentiated HCC in right lobe that shows moderately increased ^{18}F-FDG metabolism and only minimal ^{11}C-acetate activities. Right patient (C) with moderately differentiated HCC in left lobe shows dual tracer uptake. (Bottom) Transaxial sections of liver in another typical patient with HCC show 2 tumor lesions negative on ^{18}F-FDG PET but clearly identified by ^{11}C-acetate PET.

TABLE 1
Summary of 55 HCC Lesions Detected by ^{11}C-Acetate and ^{18}F-FDG in Patients of Group Ia (≤3 HCC Lesions per Patient Liver)

Lesion uptake characteristics	No. of lesions	No. of lesions	Lesion uptake characteristics
^{11}C-Acetate + and ^{18}F-FDG −*	29	7	^{18}F-FDG + and ^{11}C-acetate −*
^{11}C-Acetate + and ^{18}F-FDG +	19	19	^{18}F-FDG + and ^{11}C-acetate +
Total ^{11}C-acetate + lesions	48	26	Total ^{18}F-FDG + lesions
^{11}C-Acetate − and ^{18}F-FDG −	0	0	^{18}F-FDG − and ^{11}C-acetate −
^{11}C-Acetate sensitivity (%)	87.3	47.3	^{18}F-FDG sensitivity (%)

*Lesion is considered negative for PET tracer when it is isointense with normal liver tissue by visual inspection and is supported by lesion-to-liver SUV ratio of <1.20.

+ = Positive for PET tracer; − = negative for PET tracer.

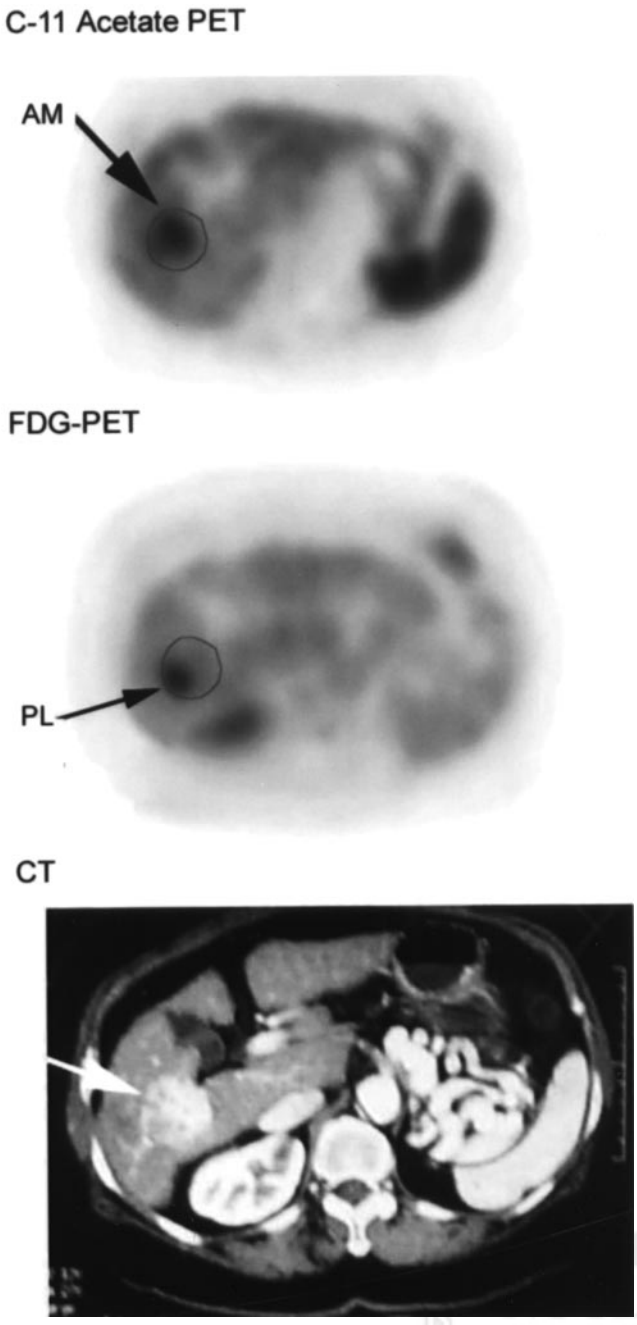

FIGURE 2. Transaxial sections of liver in patient with moderately differentiated HCC of right lobe. CT shows heterogeneous contrast enhancement within tumor. ^{11}C-Acetate PET shows focally accentuated acetate metabolism at anteromedial (AM) part of tumor, whereas ^{18}F-FDG PET shows increased glycolysis at posterolateral (PL) part of tumor. Actual boundary of tumor, mapped from CT image, is drawn to scale on ^{11}C-acetate and ^{18}F-FDG PET images.

tumor lesions were either infiltrative or poorly demarcated. In some cases, normal liver tissue could not be reliably defined. Therefore, the lesion-to-liver ratio was not calculated, and only qualitative results are discussed. We also observed that the vascular (portal or venous) metastases were more avid for ^{18}F-FDG than for ^{11}C-acetate (Fig. 4A). Extrahepatic metastasis was also more clearly demonstrated and greater in number with the ^{18}F-FDG tracer, except in a case of brain metastasis, which was detected by ^{11}C-acetate imaging but was negative on ^{18}F-FDG imaging (Fig. 4B, with surgical confirmation of metastatic moderately differentiated HCC in the right frontal lobe).

When the group Ia lesions were examined pathologically, they were categorized into 3 large groups according to cellular differentiation: well, moderate, and poor. Some tumors were reported as well-to-moderately differentiated and moderate-to-poorly differentiated. Because the pathologic categorization might have interobserver variations and there were no fine criteria between the overlapping groups, the well-to-moderately differentiated tumors were put into the well-differentiated group, and the moderate-to-poorly differentiated tumors were categorized with the poorly differentiated group for the purpose of statistical analysis. The mean lesion-to-liver SUV ratios were calculated for each group and the results are summarized in Table 2. Individual lesion-to-liver SUV ratios versus the 3 groups of differentiation are plotted in Figure 5 (sorted in descending order of ^{11}C-acetate SUV ratios within each group). Statistical analysis of the mean SUV ratios showed significant differences ($P < 0.01$ to $P < 0.0001$) between the well- and moderately differentiated groups and between the moderate and poorly differentiated groups for each tracer.

All the patients in group II (3 cholangiocarcinomas, 10 metastatic liver tumors) showed increased ^{18}F-FDG metabolism in all 16 metastatic liver lesions from colon, lung, breast, and carcinoid malignancies as well as cholangiocarcinoma (pure primary hepatic adenocarcinoma). However, no abnormal ^{11}C-acetate was detected in all of these lesions. The SUV for ^{11}C-acetate in these metastatic lesions showed no statistical difference from nontumor hepatic parenchyma ($t_{.025} \times SE \gg \mu 1 - \mu 2$ at 95% confidence). It was interesting to note within this series of study, even in the 3 cases of cholangiocarcinoma (pure primary adenocarcinoma with no HCC components), ^{11}C-acetate PET showed no abnormal uptake (Fig. 6). The specificity for ^{11}C-acetate in this group of patients was by far 100% at this stage of evaluation.

Group III patients had benign liver pathologies. Two of these patients had typical findings on MRI or CT and labeled red blood cell imaging for cavernous hemangioma. These hemangioma lesions were not metabolically distinguishable from normal hepatic parenchyma on ^{18}F-FDG PET evaluation, but they were readily identified as hypometabolic foci on ^{11}C-acetate PET imaging (partly because normal hepatic parenchyma showed more ^{11}C-acetate activity than ^{18}F-FDG activity). The patient with a single hepatic adenoma (3.2 × 3.0 cm) showed no abnormal ^{11}C-acetate or ^{18}F-FDG uptake. In the 2 patients with FNH, both had mildly increased ^{11}C-acetate uptake. One demonstrated mildly increased ^{18}F-FDG metabolism, whereas the other showed no abnormal ^{18}F-FDG uptake. The patient with the larger FNH lesion (6.2 × 5.6 cm) showed a ^{11}C-acetate

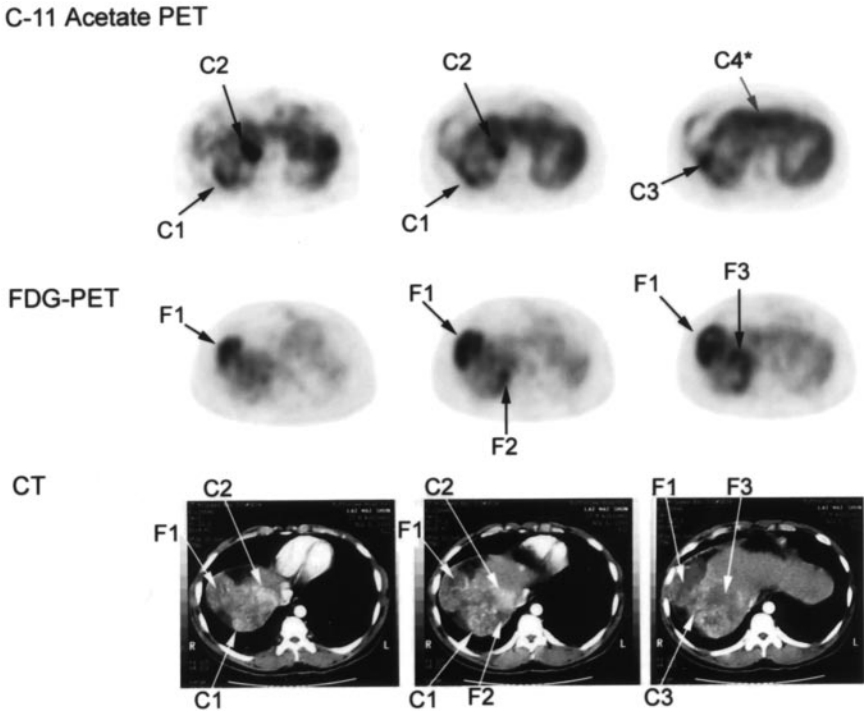

FIGURE 3. Three transaxial sections of liver in patient with multifocal HCC disease show complementary characteristics of ^{11}C-acetate and ^{18}F-FDG in PET imaging. ^{11}C-Acetate–avid tumor lesions are marked by "C" and ^{18}F-FDG–avid lesions are marked by "F."

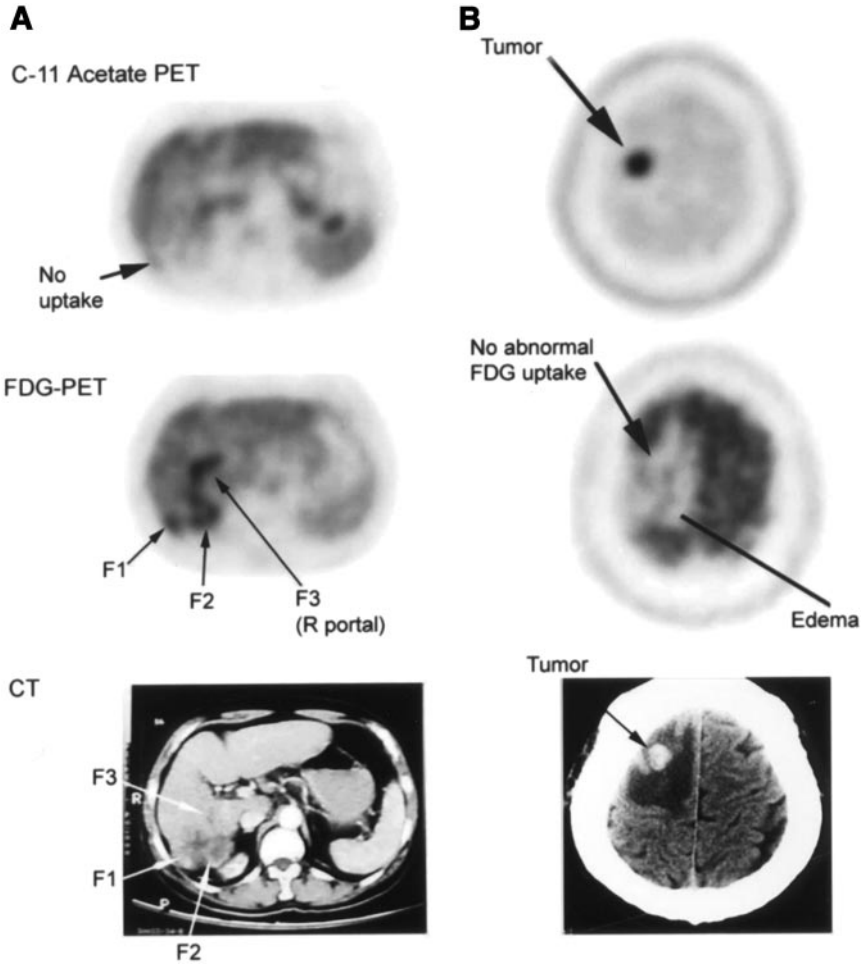

FIGURE 4. (A) Transaxial sections of liver show detection of portal metastasis by ^{18}F-FDG but not by ^{11}C-acetate PET in patient with advanced HCC and poorly differentiated tumor cells. (B) Transaxial sections of brain show metastatic nodule in right frontal lobe from primary, moderately differentiated HCC (confirmed by surgery). This is seen as lesion of increased ^{11}C-acetate metabolism but is almost completely hypometabolic on ^{18}F-FDG PET. Note surrounding edema on ^{18}F-FDG images and background of no activities in normal brain tissue on ^{11}C-acetate images.

TABLE 2
Summary of Mean Lesion-to-Liver SUV Ratios in 3 Groups of Differentiation in Group Ia HCC Lesions

Group Ia HCC lesions	^{18}F-FDG lesion-to-liver SUV ratio	^{11}C-Acetate lesion-to-liver SUV ratio
Well differentiated (n = 19)	1.09 ± 0.24	2.27 ± 0.56
Moderately differentiated (n = 24)	1.28 ± 0.26	1.62 ± 0.32
Poorly differentiated (n = 12)	2.15 ± 0.48	1.29 ± 0.39

SUV_{max} of 3.59 and a lesion-to-liver SUV ratio of 1.25 ($P <$ 0.001 in comparison with ^{11}C-acetate–avid HCC lesions). Results of the SUV and lesion-to-liver ratio for these 3 groups of patients (except group Ib) are summarized in Table 3.

DISCUSSION

In patients with a high pretest likelihood of having HCC (positive hepatitis B or C status, cirrhosis, elevated α-fetoprotein concentration), the radiologic diagnosis of HCC is usually not difficult to make. It is related partly to the fact that today the incidence of benign hepatic lesions such as FNH and adenoma is rather low, and, in fact, FNH is frequently an entity diagnosed by exclusion because of the concern of biopsy sampling error. However, various trials and combinations of techniques regarding different imaging methods exist in the literature in an attempt to increase the accuracy of detecting and diagnosing atypical lesions and tumors of <2-cm size (*19–25*). This is particularly true in patients with a low or intermediate likelihood of having the disease (negative status of hepatitis B surface antigen, borderline or normal α-fetoprotein concentration).

Cirrhosis is another known variable that causes confounding degrees of contrast-enhanced appearances on both conventional and helical CT (*26–28*), primarily related to the coexistence of regenerating and dysplastic nodules. Peterson and Baron (*27*) reported a low detection accuracy of 37%–45% based on recent screening studies on large cirrhotic populations. In those patients with cirrhotic livers and small lesions, the diagnosis of HCC can be difficult to make.

The role of ^{18}F-FDG PET in the detection and diagnosis of HCC is well known to be very limited. Okazumi et al. (*11*) proposed that HCC may be classified into 3 "metabolic" types according to the avidity of the tumor cells for ^{18}F-FDG. The net accumulation of ^{18}F-FDG-6-phosphate is determined both by the phosphorylation kinase activity (reflected by the kinetic rate constant $k_{3)}$ and by the abundance of the glucose-6-phosphatase activity (k_4). In many forms of tumor tissue, ^{18}F-FDG is "metabolically trapped" because ^{18}F-FDG-6-phosphate can neither pass on to the next step of glycolysis nor back diffuse to the circulation because of the low concentration of glucose-6-phosphatase enzyme (k_4 ap-

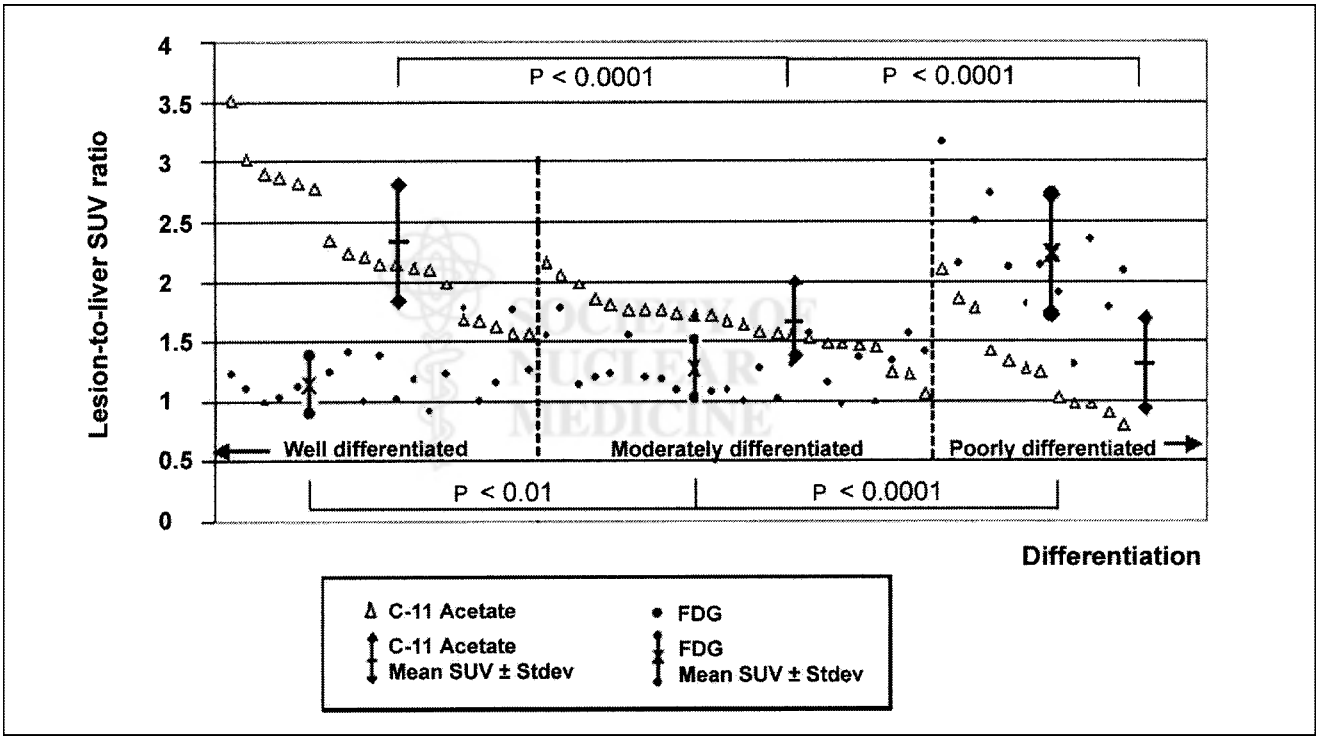

FIGURE 5. Composite chart plots lesion-to-liver SUV ratio of all HCC lesions for patients in group Ia (with ≤3 HCC lesions) against 3 large groups of cellular differentiation. There is no fine line of transition between grades of differentiation; dashed vertical line represents rough transitional zone of visual grading reported by pathologists. Each set of vertical data points is paired: △, ^{11}C-acetate; ●, ^{18}F-FDG. Values are sorted in descending order of ^{11}C-acetate SUV ratios in each group.

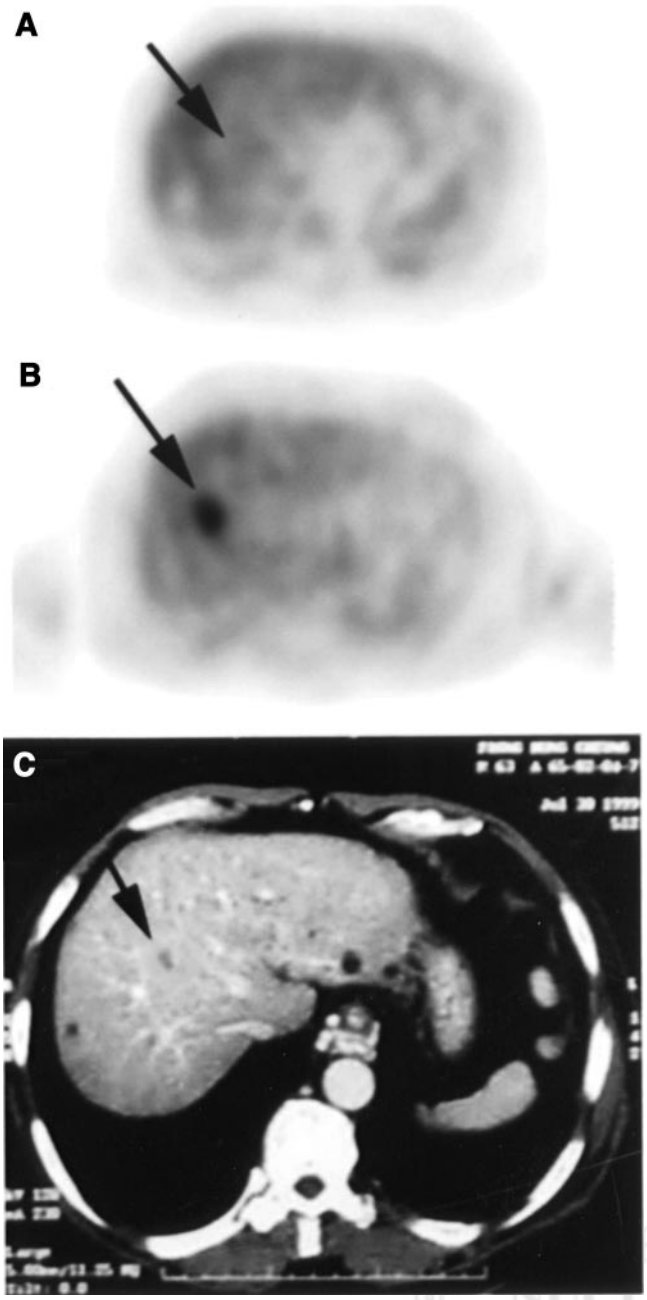

FIGURE 6. Transaxial ^{11}C-acetate PET (A), ^{18}F-FDG PET (B), and CT (C) sections of patient with cholangiocarcinoma (pure adenocarcinoma) show no abnormal ^{11}C-acetate metabolism but show increased ^{18}F-FDG activity within tumor.

proaches zero). In normal liver parenchyma, the concentration of glucose-6-phosphatase is relatively high (nonzero k_4). This actually may account for the fact that the intensity of normal liver is only mild on ^{18}F-FDG PET imaging (SUV usually ~2.0), contrary to its role as the powerhouse of the human body. Okazumi et al. found that the type 1 hepatocellular carcinoma cells have a lower k_4/k_3 ratio and may show increased uptake on ^{18}F-FDG PET imaging like many other forms of malignancy. Type 2 hepatocellular carcinoma cells have a k_4/k_3 ratio similar to that of normal hepatocytes and therefore may be isointense on ^{18}F-FDG PET imaging. Type 3 tumor cells have a higher k_4/k_3 ratio and are actually hypointense. The combination of type 2 and type 3 tumors constitutes about a 43% false-negative rate in Okazumi's group. In our study, the false-negative rate by account of tumor lesions is 52.7%, slightly higher than their reported value as well as those by others (*6,10*).

In fact, the degree and nature of tumor cell differentiation are known to affect the amount of ^{18}F-FDG accumulation in cells, as suggested by other investigators with smaller samples in their studies (*8,12,14*). Early research on rat hepatomas had suggested that the patterns of glycolytic enzymes might reflect hepatoma cell growth, function, and graded dedifferentiation (*29*). Because well-differentiated hepatocellular carcinoma cells are histologically closer to the normal liver cells than to the undifferentiated types, the abundance of glucose-6-phosphatase enzyme may render these tumors undetectable. This relationship is strongly suggested by data in this study. Figure 5 shows that there is a statistically significant relationship of cellular differentiation with the tumor's avidity for ^{18}F-FDG and ^{11}C-acetate metabolism in terms of the lesion-to-liver SUV ratio. The well-differentiated and well-to-moderately differentiated types tend to be negative for ^{18}F-FDG; whereas the poorly differentiated and moderate-to-poorly differentiated types show increased ^{18}F-FDG metabolism.

The use of ^{11}C-acetate in tumor imaging has been suggested recently in urologic malignancies (*15,16*). Possible biochemical paths of acetate incorporation or accumulation include (a) entering the Krebs cycle from acetyl coenzyme A (acetyl CoA) or as an intermediate metabolite, (b) esterification to form acetyl CoA as a major precursor in β-oxidation for fatty acid synthesis, (c) combining with glycine in heme synthesis, and (d) through citrate for cholesterol synthesis. Of all of these possible metabolic pathways, participation in free fatty acid (lipid) synthesis is believed to be the dominant method of incorporation in tumors. Yoshimoto et al. (*30*) suggested that this mechanism of tumor uptake was different from that of myocardium, in which ^{11}C-acetate was channeled mainly to the Krebs cycle. The results of this study suggest that ^{11}C-acetate is able to detect the entire proportion of HCC lesions that are negative on ^{18}F-FDG imaging. In those tumors that are both ^{11}C-acetate and ^{18}F-FDG positive (the moderately differentiated type), some cases suggest that these tracers are taken up by different parts of the tumor (Figs. 2 and 3). Therefore, mixed metabolic constituents and kinetics are likely to be present within the same tumor at variable degrees. These 2 tracers are probably complementary to each other in the detection of HCC. The lesion-to-liver SUV ratios for ^{11}C-acetate and ^{18}F-FDG have a statistically significant relationship to each other in tumor cellular differentiation (Fig. 5). In the detection of individual tumor lesions (partial or whole tumor), the overall ability of ^{11}C-acetate is better than that of ^{18}F-FDG, with a detection sensitivity of 87.3% versus 47.3% using ^{18}F-FDG. This relative accuracy appears to be highly de-

TABLE 3
Summary of SUV and Lesion-to-Liver SUV Ratio for Individual Group Lesions in ^{18}F-FDG and ^{11}C-Acetate Metabolism

Group	No. of patients	No. of lesions	^{18}F-FDG*		^{11}C-Acetate*	
			SUV_{max}	Lesion-to-liver ratio	SUV_{max}	Lesion-to-liver ratio
Ia (≤3 HCC lesions)†	32	55	3.51 ± 1.38	1.45 ± 0.49	7.33 ± 2.02	1.96 ± 0.63
II (non-HCC malignant lesions)	13	16	6.25 ± 1.62	2.81 ± 0.78	3.84 ± 0.48	0.98 ± 0.04
III (benign lesions)	5	10	2.21 ± 0.46	0.99 ± 0.25	3.27 ± 0.37	0.93 ± 0.30

*Mean ± SD.
†Group Ib patients (n = 7) are not tabulated because they have diffuse or multifocal metastasis. Many lesions could not be clearly demarcated, and some diffusely infiltrative types were difficult to differentiate from nontumor liver tissue.

pendent on tumor cellular differentiation. For HCC with ≤3 tumor lesions, tumor cells show a variable degree of differentiation with 60%–70% in the well- and moderately differentiated category. As tumor cells become more aggressive in later or advanced stages, cellular kinetic also change. The poor- or less well-differentiated tumor cells begin to retain ^{18}F-FDG. In our study, all of the group Ib patients showed more ^{18}F-FDG accumulation in their primary liver tumors and metastases, including vascular, nodal and distant metastases (except 1 case with a surgically confirmed moderately differentiated brain metastasis, as depicted in Fig. 4). Furthermore, the finding of a strong complementary relationship of ^{11}C-acetate and ^{18}F-FDG in the evaluation of HCC appears to be very important to the use of PET imaging in the monitoring of therapy in patients with this tumor.

The other interesting observation is that ^{11}C-acetate may be quite specific for HCC in the evaluation of liver lesions. Our study showed that ^{11}C-acetate is negative in hemangioma; cholangiocarcinoma (pure primary adenocarcinoma of liver without HCC components); secondary carcinomas from colon, breast, and lung; as well as carcinoid tumors. This specificity can be highly useful in the preliminary evaluation of unknown liver masses. When both tracers are positive or positive only for ^{11}C-acetate, the likelihood for the tumor mass to be HCC is very high. On the other hand, when a liver mass is positive only for ^{18}F-FDG but is negative for ^{11}C-acetate, the possibility of non-HCC malignancy or poorly differentiated HCC should be considered. In case both tracers are negative, benign pathology is more likely. Two cases of FNH showed only mildly increased ^{11}C-acetate metabolism. The lesion with the higher lesion-to-liver SUV ratio showed a value of 1.25, statistically lower than the average value of all of the ^{11}C-acetate–positive HCC cases in this study (1.96 ± 0.63; $P < 0.001$).

It is not possible to include all other liver lesions in a single study; therefore, we studied only 2 FNH cases and 1 case of adenoma. In addition, other pathology such as fibrolamellar HCC and liver abscess have not yet been studied. In the next stage of evaluation, patients with smaller HCC lesions of <2-cm size and more severely cirrhotic livers may be investigated. The findings reported here and concurrent work on the kinetic modeling of ^{11}C-acetate in HCC may add to the understanding of the molecular basis of this tumor. A reliable diagnostic PET radiopharmaceutical is important for formulating and monitoring therapeutic treatment of this tumor.

CONCLUSION

HCC is a malignancy of high prevalence and grave prognosis. In this prospective study, our preliminary data have shown that ^{11}C-acetate PET not only is significantly more sensitive than ^{18}F-FDG PET in the detection of individual HCC lesions but also appears to be quite specific. Our findings also suggest that tumor detection by these 2 tracers is dependent on histologic differentiation. Therefore, ^{11}C-acetate may likely be a promising tracer in complementing the deficiency of ^{18}F-FDG in PET imaging of liver masses.

ACKNOWLEDGMENTS

The authors thank the Hospital Board of the Hong Kong Sanatorium and Hospital for their support of this work, Jacky Cheung and Kin-Chung Liu for preparation of the PET radiopharmaceuticals, May Chan and the technologists for clinical assistance, and Maria Yeung and Jennifer Choi for finalizing this manuscript.

REFERENCES

1. el-Serag H. Epidemiology of hepatocellular carcinoma. *Clin Liver Dis.* 2001;5: 87–107
2. Okano H, Shiraki K, Inoue H, et al. Comparison of screening methods for hepatocellular carcinomas in patients with cirrhosis. *Anticancer Res.* 2001;21: 2979–2982.
3. Fracanzani AL, Burdick L, Borzio M, et al. Contrast-enhanced Doppler ultrasonography in the diagnosis of hepatocellular carcinoma and premalignant lesions in patients with cirrhosis. *Hepatology.* 2001;34:1109–1112.
4. Harvey CJ, Albrecht T. Ultrasound of focal liver lesions. *Eur Radiol.* 2001;11: 1578–1593.
5. Braga F, Flamen P, Mortelmans L, et al. Ga-67-positive and F-18 FDG-negative imaging in well-differentiated hepatocellular carcinoma. *Clin Nucl Med.* 2001; 26:642.
6. Delbeke D, Martin W, Sandler M, et al. Evaluation of benign vs malignant hepatic lesions with positron emission tomography. *Arch Surg.* 1998;133:510–515.
7. Fukunaga T, Enomoto K, Okazumi S, et al. Evaluation of gastroenterological

disease by using ^{18}F-FDG PET: differential diagnosis of malignancy from benignity. *Kaku Igaku.* 1992;29:687–690.
8. Goldberg M, Lee M, Fischman A, et al. Fluorodeoxyglucose PET of abdominal and pelvic neoplasms: potential role in oncologic imaging. *Radiographics.* 1993; 13:1047–1062.
9. Iwata Y, Shiomi S, Sasaki N, et al. Clinical usefulness of positron emission tomography with fluorine-18-fluorodeoxyglucose in the diagnosis of liver tumors. *Ann Nucl Med.* 2000;14:121–126.
10. Khan M, Combs C, Brunt E, et al. Positron emission tomography scanning in the evaluation of hepatocellular carcinoma. *J Hepatol.* 2000;32:792–797.
11. Okazumi S, Isono K, Enomoto K, et al. Evaluation of liver tumors using fluorine-18-fluorodeoxyglucose PET: characterization of tumor and assessment of effect of treatment. *J Nucl Med.* 1992;33:333–339.
12. Schroder O, Trojan J, Zeuzem S, et al. Limited value of fluorine-18-fluorodeoxyglucose PET for the differential diagnosis of focal liver lesions in patients with chronic hepatitis C virus infection. *Nuklearmedizin.* 1998;37:279–285.
13. Torizuka T, Tamaki N, Inokuma T, et al. Value of fluorine-18-FDG-PET to monitor hepatocellular carcinoma after interventional therapy. *J Nucl Med.* 1994; 35:1965–1969.
14. Trojan J, Schroeder O, Raedle J, et al. Fluorine-18 FDG positron emission tomography for imaging of hepatocellular carcinoma. *Am J Gastroenterol.* 1999; 94:3314–3319.
15. Oyama N, Akino H, Kanamaru H, et al. ^{11}C-Acetate PET imaging of prostate cancer. *J Nucl Med.* 2002;43:181–186.
16. Shreve P, Chiao PC, Humes HD, et al. Carbon-11-acetate PET imaging in renal disease. *J Nucl Med.* 1995;36:1595–1601.
17. Norenberg JP, Simpson NR, Dunn BB, et al. Remote synthesis of [^{11}C] acetate. *Appl Radiat Isot.* 1992;43:943–945.
18. Hamacher K, Coenen HH, Stocklin G. Efficient stereospecific synthesis of no-carrier-added 2-[^{18}F]-fluoro-2-deoxy-D-glucose using aminopolyether supported nucleophilic substitution. *J Nucl Med.* 1986;27:235–238.
19. Tateishi Y. Diagnosis of 26 small hepatocellular carcinoma using incremental dynamic computed tomography. *Kurume Med J.* 1997;44:321–326.
20. Takayasu K, Furukawa H, Wakao F, et al. CT diagnosis of early hepatocellular carcinoma: sensitivity, findings, and CT-pathologic correlation. *AJR.* 1995;164: 885–890.
21. Murakami T, Kim T, Takamura M, et al. Hypervascular hepatocellular carcinoma: detection with double arterial phase multi-detector row helical CT. *Radiology.* 2001;218:763–767.
22. Lencioni R, Pinto F, Armillotta N, et al. Intrahepatic metastatic nodules of hepatocellular carcinoma detected at lipiodol-CT: imaging-pathologic correlation. *Abdom Imaging.* 1997;22:253–258.
23. Hann L, Winston C, Brown K, et al. Diagnostic imaging approaches and relationship to hepatobiliary cancer staging and therapy. *Semin Surg Oncol.* 2000; 19:94–115.
24. Hanafusa K, Ohashi I, Gomi N, et al. Differential diagnosis of early homogeneously enhancing hepatocellular carcinoma and hemangioma by two-phase CT. *J Comput Assist Tomogr.* 1997;21:361–368.
25. Rode A, Bancel B, Douek P, et al. Small nodule detection in cirrhotic livers: evaluation with US, spiral CT, and MRI and correlation with pathologic examination of explanted liver. *J Comput Assist Tomogr.* 2001;25:327–336.
26. Coakley FV, Schwartz LH. Imaging of hepatocellular carcinoma: a practical approach. *Semin Oncol.* 2001;28:460–473.
27. Peterson MS, Baron RL. Radiologic diagnosis of hepatocellular carcinoma. *Clin Liver Dis.* 2001;5:123–144.
28. Zardi EM, Uwechie V, Picardi A, et al. Liver focal lesions and hepatocellular carcinoma in cirrhotic patients: from screening to diagnosis. *Clin Ter.* 2001;152: 185–188.
29. Shonk CE, Morris HP, Boxer GE. Patterns of glycolytic enzymes in rat liver and hepatoma. *Cancer Res.* 1965;25:671–676.
30. Yoshimoto M, Waki A, Yonekura Y, et al. Characterization of acetate metabolism in tumor cells in relation to cell proliferation: acetate metabolism in tumor cells. *Nucl Med Biol.* 2001;28:117–122.